



*Supplement of*

## **Impact of temperature on the role of Criegee intermediates and peroxy radicals in dimer formation from $\beta$ -pinene ozonolysis**

**Yiwei Gong et al.**

*Correspondence to:* Yiwei Gong (yiwei.gong@kit.edu) and Harald Saathoff (harald.saathoff@kit.edu)

The copyright of individual parts of the supplement might differ from the article licence.

### **Calibration of FIGAERO-CIMS with pinic acid**

- 15 Pinic acid, as the most abundant product formed during the reaction, was utilized to characterize the sensitivity of CIMS. Pinic acid ( $C_9H_{14}O_4$ , 92%, Chemspace) was dissolved into methanol to  $1.77 \times 10^{-4}$ ,  $1.77 \times 10^{-5}$ , and  $1.77 \times 10^{-6} \text{ g mL}^{-1}$  as standard solutions. Different volumes of the standard solutions were deposited on a PTFE filter using a syringe. The filter was heated by FIGAREO-CIMS in ultra-high-purity nitrogen following a thermal desorption procedure. The results are shown in Fig. S2.

20

### **SOA density calculation**

Effective density of aerosol was derived from comparing the mass distribution versus vacuum aerodynamic diameter from

25 AMS, and the size distribution versus mobility diameter from SMPS. Considering that these newly formed particles during reaction were usually smaller than 70 nm, which could not be measured by AMS, the effective density calculated here relied on the organics that partitioned to the inorganic seed particles.

**Table S1. SOA yields and reaction conditions in  $\beta$ -pinene ozonolysis studies.**

Temperature (K)	RH (%)	OH scavenger	Aerosol mass ( $\mu\text{g}\cdot\text{m}^{-3}$ )	SOA yield (%)	Reference
263–303	<0.03	none	2–284	3–39	von Hessberg et al., 2009
300	22	none	156 ± 3	18 ± 1	Xu et al., 2021
293	6.3	cyclohexane	174 ± 3	17 ± 1	Lee et al., 2006
306–307	–	2-butanol	11–19	4–8	Yu et al., 1999
248–298	<0.01	CO	18–25	11–19	This work

**Table S2.** T<sub>max</sub> (°C) of all the monomers and dimers at different temperatures.

	298 K	273 K	248 K		298 K	273 K	248 K		298 K	273 K	248 K
C8H8O3	75.5	54	66.3	C16H22O7	115	88.3	83	C18H26O9	115	102.5	95.4
C8H8O4	115	68.1	50.5	C16H22O8	116.7	115	83	C18H26O10	116.7	99	97.2
C8H8O5	115	48.8	125.3	C16H22O9	120	104.3	97.2	C18H26O11	107.8	102.5	102.5
C8H8O6	81.1	57.4	55.8	C16H22O10	118.4	107.8	107.8	C18H28O4	109.7	109.7	61
C8H10O3	120	115	64.6	C16H24O4	113.2	107.8	100.8	C18H28O6	91.8	93.6	88.3
C8H10O4	62.8	43.9	43.9	C16H24O5	115	107.8	77.2	C18H28O7	118.4	62.8	61
C8H10O5	61	43.9	42.4	C16H24O6	84.7	75.5	75.5	C18H28O8	121.9	113.2	106
C8H10O6	83	59.2	42.4	C16H24O7	116.7	93.6	100.8	C18H28O9	113.2	102.5	93.6
C8H10O8	99	50.5	99	C16H24O8	111.5	107.8	104.3	C18H28O11	125.3	116.7	115
C8H10O9	102.5	50.5	50.5	C16H24O9	115	111.5	102.5	C18H30O4	84.7	91.8	57.4
C8H10O10	75.5	118.4	142.8	C16H24O10	107.8	102.5	77.2	C18H30O5	111.5	109.7	84.7
C8H12O3	75.5	71.8	79.1	C16H24O11	99	95.4	69.8	C18H30O6	104.3	109.7	88.3
C8H12O4	111.5	111.5	109.7	C16H24O12	109.7	164.4	95.4	C18H30O7	106	109.7	106
C8H12O5	69.8	36.5	54	C16H26O4	106	73.6	81.1	C18H30O8	116.7	111.5	109.7
C8H12O6	84.7	54	54	C16H26O5	115	109.7	71.8	C18H30O9	107.8	100.8	95.4
C8H12O7	81.1	57.4	48.8	C16H26O6	86.6	83	73.6	C18H30O11	121.9	120	115
C8H12O8	71.8	95.4	55.8	C16H26O7	106	107.8	99	C18H30O12	118.4	121.9	116.7
C8H14O3	102.5	102.5	73.6	C16H26O8	113.2	107.8	102.5	C18H32O8	115	109.7	95.4
C8H14O4	79.1	33.7	36.5	C16H26O9	106	99	93.6	C18H32O9	109.7	115	100.8
C8H14O5	71.8	62.8	54	C16H26O10	113.2	102.5	95.4	C18H32O10	116.7	102.5	83
C8H14O6	75.5	59.2	57.4	C16H26O11	116.7	111.5	95.4	C18H32O11	121.9	116.7	109.7
C8H14O7	73.6	118.4	59.2	C16H26O12	120	104.3	180.5	C18H32O12	118.4	116.7	109.7
C8H14O8	118.4	115	104.3	C16H28O4	71.8	104.3	84.7	C18H34O4	104.3	99	77.2
C8H16O3	73.6	73.6	66.3	C16H28O5	100.8	71.8	77.2	C18H34O6	111.5	109.7	106
C8H16O4	93.6	41	55.8	C16H28O6	109.7	111.5	106	C18H34O9	111.5	113.2	118.4
C8H16O5	75.5	59.2	52.3	C16H28O7	106	113.2	95.4	C18H34O10	115	107.8	95.4
C8H16O6	66.3	69.8	195.3	C16H28O8	107.8	102.5	100.8	C18H34O11	113.2	113.2	99
C8H16O7	116.7	73.6	68.1	C16H28O11	118.4	106	102.5	C18H36O9	113.2	111.5	102.5
C9H8O4	54	200.4	123.7	C16H30O4	90	109.7	62.8	C19H24O7	118.4	115	100.8
C9H8O5	116.7	50.5	86.6	C16H30O5	116.7	77.2	99	C19H24O8	116.7	118.4	170.9
C9H8O6	115	91.8	55.8	C16H30O8	104.3	111.5	93.6	C19H24O10	115	106	48.8
C9H8O7	118.4	113.2	121.9	C16H30O10	116.7	116.7	91.8	C19H24O11	120	115	106
C9H10O4	125.3	50.5	200	C16H30O12	120	111.5	111.5	C19H26O5	104.3	99	95.4
C9H10O5	144.4	151.1	99	C16H32O7	84.7	64.6	57.4	C19H26O8	113.2	115	77.2
C9H10O6	100.8	57.4	71.8	C17H22O5	106	81.1	100.8	C19H26O9	116.7	95.4	109.7
C9H10O7	77.2	77.2	55.8	C17H22O6	73.6	77.2	86.6	C19H26O11	115	100.8	86.6
C9H10O8	79.1	59.2	54	C17H22O7	118.4	93.6	99	C19H28O4	106	106	62.8
C9H10O9	81.1	73.6	102.5	C17H22O8	111.5	99	52.3	C19H28O6	97.2	95.4	88.3
C9H10O10	93.6	107.8	179.1	C17H22O9	109.7	102.5	102.5	C19H28O7	116.7	102.5	79.1
C9H12O3	115	68.1	61	C17H24O4	102.5	97.2	69.8	C19H28O8	102.5	100.8	91.8
C9H12O4	118.4	100.8	62.8	C17H24O5	113.2	111.5	71.8	C19H28O9	115	109.7	88.3
C9H12O5	79.1	79.1	55.8	C17H24O6	113.2	111.5	59.2	C19H28O10	106	91.8	109.7
C9H12O6	93.6	91.8	77.2	C17H24O7	115	107.8	107.8	C19H30O4	102.5	77.2	62.8
C9H12O7	81.1	57.4	55.8	C17H24O8	116.7	59.2	55.8	C19H30O5	111.5	69.8	69.8
C9H12O8	95.4	73.6	73.6	C17H24O9	116.7	107.8	104.3	C19H30O6	93.6	66.3	75.5
C9H12O9	104.3	125.3	125.3	C17H24O10	113.2	102.5	84.7	C19H30O7	88.3	88.3	84.7

C9H14O3	83	99	61	C17H24O11	118.4	100.8	199.8	C19H30O8	95.4	79.1	79.1
C9H14O4	111.5	43.9	62.8	C17H26O4	81.1	84.7	68.1	C19H30O9	100.8	100.8	88.3
C9H14O5	75.5	64.6	50.5	C17H26O5	90	88.3	71.8	C19H30O10	111.5	106	115
C9H14O6	79.1	57.4	52.3	C17H26O6	86.6	91.8	88.3	C19H30O11	123.7	120	100.8
C9H14O7	71.8	54	54	C17H26O7	113.2	111.5	86.6	C19H32O4	99	99	62.8
C9H14O8	83	57.4	54	C17H26O8	107.8	107.8	104.3	C19H32O5	97.2	90	59.2
C9H14O10	75.5	197	194.7	C17H26O9	118.4	113.2	106	C19H32O6	113.2	66.3	57.4
C9H16O3	109.7	107.8	106	C17H26O10	107.8	99	99	C19H32O7	113.2	107.8	102.5
C9H16O4	26.5	26.5	26.5	C17H26O11	107.8	106	106	C19H32O8	106	102.5	64.6
C9H16O5	99	59.2	47.3	C17H28O4	109.7	79.1	75.5	C19H32O12	115	113.2	115
C9H16O6	68.1	61	47.3	C17H28O5	84.7	75.5	75.5	C19H34O8	109.7	107.8	95.4
C9H16O7	83	81.1	61	C17H28O6	106	100.8	81.1	C19H34O10	118.4	116.7	99
C9H18O3	81.1	75.5	64.6	C17H28O7	107.8	107.8	104.3	C19H34O12	120	109.7	118.4
C10H10O5	116.7	120	59.2	C17H28O8	115	109.7	109.7	C19H36O4	93.6	111.5	106
C10H10O6	116.7	93.6	50.5	C17H28O9	100.8	100.8	64.6	C19H36O7	102.5	102.5	200.1
C10H10O7	120	52.3	41	C17H28O10	118.4	132.4	99	C19H36O8	116.7	116.7	95.4
C10H12O4	118.4	109.7	81.1	C17H28O11	121.9	118.4	100.8	C19H36O9	118.4	95.4	99
C10H12O5	109.7	113.2	199.8	C17H28O12	113.2	102.5	104.3	C19H36O10	115	111.5	100.8
C10H12O6	77.2	62.8	91.8	C17H30O4	97.2	111.5	68.1	C19H36O11	111.5	113.2	102.5
C10H12O7	79.1	100.8	61	C17H30O5	88.3	77.2	69.8	C19H36O12	120	115	88.3
C10H12O8	81.1	93.6	81.1	C17H30O8	106	109.7	102.5	C19H38O10	115	104.3	107.8
C10H12O9	115	66.3	151.1	C17H30O9	111.5	111.5	100.8	C20H22O10	127.2	123.7	195.8
C10H14O3	95.4	69.8	64.6	C17H30O10	116.7	115	106	C20H26O7	111.5	106	84.7
C10H14O4	154.6	99	106	C17H30O12	121.9	111.5	125.3	C20H28O6	115	100.8	199.8
C10H14O5	93.6	77.2	64.6	C17H32O4	86.6	81.1	81.1	C20H28O7	109.7	109.7	106
C10H14O6	75.5	61	61	C17H32O5	102.5	113.2	95.4	C20H30O6	104.3	99	90
C10H14O7	86.6	52.3	61	C17H32O6	116.7	99	97.2	C20H30O8	91.8	86.6	102.5
C10H14O8	83	84.7	42.4	C17H32O7	113.2	111.5	104.3	C20H30O10	116.7	107.8	90
C10H14O9	71.8	62.8	75.5	C17H32O9	120	100.8	91.8	C20H30O11	120	104.3	102.5
C10H14O10	75.5	156.3	41	C17H32O10	102.5	115	106	C20H32O5	91.8	100.8	79.1
C10H16O3	109.7	116.7	57.4	C17H32O11	107.8	100.8	104.3	C20H32O6	88.3	93.6	64.6
C10H16O4	84.7	68.1	62.8	C17H32O12	116.7	106	88.3	C20H32O7	104.3	102.5	79.1
C10H16O5	97.2	62.8	68.1	C17H34O5	107.8	113.2	73.6	C20H32O8	107.8	100.8	97.2
C10H16O6	71.8	59.2	61	C17H34O9	107.8	107.8	100.8	C20H32O9	109.7	107.8	90
C10H16O7	84.7	68.1	57.4	C17H34O11	106	111.5	100.8	C20H32O10	116.7	109.7	115
C10H16O8	84.7	73.6	99	C18H22O9	113.2	109.7	111.5	C20H32O11	111.5	106	116.7
C10H16O10	118.4	115	121.9	C18H24O7	111.5	93.6	91.8	C20H34O6	86.6	97.2	81.1
C10H18O3	88.3	107.8	107.8	C18H24O8	120	107.8	88.3	C20H34O8	99	86.6	104.3
C10H18O4	90	68.1	41	C18H24O9	121.9	102.5	99	C20H34O9	113.2	107.8	93.6
C10H18O5	90	41	64.6	C18H26O4	90	83	71.8	C20H34O10	111.5	121.9	102.5
C10H18O6	59.2	61	59.2	C18H26O5	107.8	68.1	66.3	C20H38O9	113.2	109.7	83
C10H18O7	68.1	61	59.2	C18H26O6	106	100.8	55.8	C20H40O9	109.7	113.2	104.3
C10H18O8	109.7	97.2	71.8	C18H26O7	115	93.6	77.2	C20H40O11	118.4	116.7	97.2
C16H22O5	102.5	88.3	75.5	C18H26O8	118.4	93.6	81.1				

40 **Table S3. The molar yields of HCHO and nopolone in  $\beta$ -pinene ozonolysis studies.**

Temperature (K)	OH scavenger	RH (%)	HCHO	Nopolone	Reference
296±2	cyclohexane	dry	0.65±0.04	0.16±0.04	Winterhalter et al., 2000
293	cyclohexane	6.3	0.65±0.06	0.17±0.02	Lee et al., 2006
295±4	cyclohexane	dry	—	0.16±0.03	Ma and Marston, 2008
306–307	2-butanol	—	—	0.16–0.17	Yu et al., 1999
248–298	CO	<0.01	0.63±0.06	0.16±0.02	This study

**Table S4. Updates to the formation of  $\beta$ -pinene-derived Criegee intermediates suggested for MCM v3.3.1.**

No.	Modified reaction	Branching ratio in MCM	Updated branching ratio	Reference
1	BPINENE + O <sub>3</sub> →NOPINONE + CH <sub>2</sub> OOF	0.40	0.20	Ma and Marston, 2008; Nguyen et al., 2009; This work
2	BPINENE + O <sub>3</sub> →NOPINOAA + HCHO	0.60	0.80	Ma and Marston, 2008; Nguyen et al., 2009; This work
3	CH <sub>2</sub> OOF→CH <sub>2</sub> OO	0.37	0.50	Ahrens et al., 2014; Winterhalter et al., 2000; Zhang and Zhang, 2005
4	CH <sub>2</sub> OOF→HO <sub>2</sub> +CO+OH	0.13	0.30	Atkinson et al., 1992; Nguyen et al., 2009
5	CH <sub>2</sub> OOF→CO	0.50	0.20	This work
6	NOPINOAA→NOPINOO	0.17	0.40	Ahrens et al., 2014; Winterhalter et al., 2000; Zhang and Zhang, 2005
7	NOPINOAA→NOPINDO <sub>2</sub> + OH	0.50	0.30	Atkinson et al., 1992; Nguyen et al., 2009
8	NOPINOAA→C <sub>8</sub> BC	0.33	0.30	This work

## References

- Ahrens, J., Carlsson, P. T. M., Hertl, N., Olzmann, M., Pfeifle, M., Wolf, J. L., and Zeuch, T.: Infrared Detection of Criegee  
50 Intermediates Formed during the Ozonolysis of  $\beta$ -Pinene and Their Reactivity towards Sulfur Dioxide, *Angew. Chem. Int.*  
Ed., 53, 715–719, doi: 10.1002/anie.201307327, 2014.
- Atkinson, R., Aschmann, S. M., Arey, J., and Shorees, B.: Formation of OH radicals in the gas phase reactions of O<sub>3</sub> with a  
series of terpenes, *J. Geophys. Res.*, 97, 6065–6073, doi: 10.1029/92JD00062, 1992.
- Lee, A., Goldstein, A. H., Keywood, M. D., Gao, S., Varutbangkul, V., Bahreini, R., Ng, N. L., Flagan, R. C., and Seinfeld, J.  
55 H., Gas-phase products and secondary aerosol yields from the ozonolysis of ten different terpenes, *J. Geophys. Res. Atmos.*,  
111, D07302, doi: 10.1029/2005JD006437, 2006.
- Ma, Y. and Marston, G.: Multifunctional acid formation from the gas-phase ozonolysis of  $\beta$ -pinene, *Phys. Chem. Chem.*  
Phys., 10, 6115–6126, doi: 10.1039/b807863g, 2008.
- Nguyen, T., Peeters, J., and Vereecken, L.: Theoretical study of the gas-phase ozonolysis of  $\beta$ -pinene (C<sub>10</sub>H<sub>16</sub>), *Phys. Chem.*  
60 *Chem. Phys.*, 11, 5643–5656, doi: 10.1039/b822984h, 2009.
- von Hessberg, C., von Hessberg, P., Pöschl, U., Bilde, M., Nielsen, O. J., and Moortgat, G. K.: Temperature and humidity  
dependence of secondary organic aerosol yield from the ozonolysis of  $\beta$ -pinene, *Atmos. Chem. Phys.*, 9, 3583–3599, doi:  
10.5194/acp-9-3583-2009, 2009.
- Winterhalter, R., Neeb, P., Grossmann, D., Kolloff, A., Horie, O., and Moortgat, G.: Products and Mechanism of the Gas  
65 Phase Reaction of Ozone with  $\beta$ -Pinene, *J. Atmos. Chem.*, 35, 165–197, doi: 10.1023/A:1006257800929, 2000.
- Xu, L., Yang, Z. M., Tsona, N. T., Wang, X. K., George, C., and Du, L.: Anthropogenic–biogenic interactions at night:  
Enhanced formation of secondary aerosols and particulate nitrogen- And sulfur-containing organics from  $\beta$ -pinene oxidation,  
Environ. Sci. Technol., 55, 7794–7807, doi: 10.1021/acs.est.0c07879, 2021.
- Yu, J., Cocker, D. R., Griffin, R. J., Flagan, R. C., and Seinfeld, J. H.: Gas-Phase ozone oxidation of monoterpenes: gaseous  
70 and particulate products, *J. Atmos. Chem.*, 34, 207–258, doi: 10.1023/A:100625493058, 1999.
- Zhang, D. and Zhang, R. Y.: Ozonolysis of  $\alpha$ -pinene and  $\beta$ -pinene: Kinetics and mechanism, *J. Chem. Phys.*, 122, 114308,  
doi: 10.1063/1.1862616, 2005.

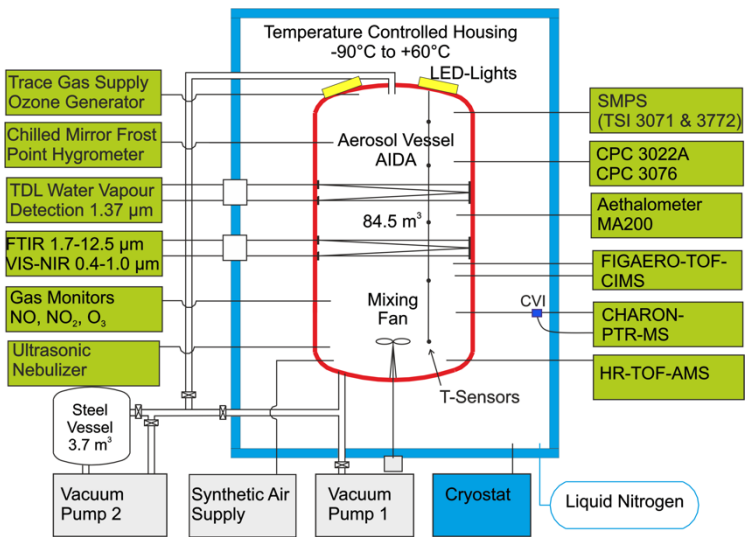


**Figure S1. Schematic of the AIDA simulation chamber with the typical instrumentation.**

80

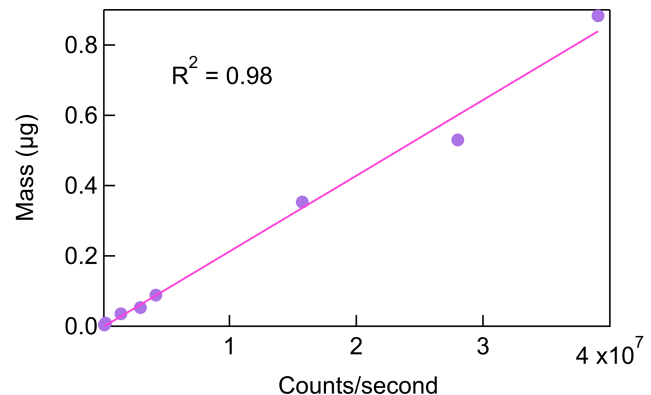


**Figure S2. Calibration of the FIGAERO-CIMS with pinic acid.**

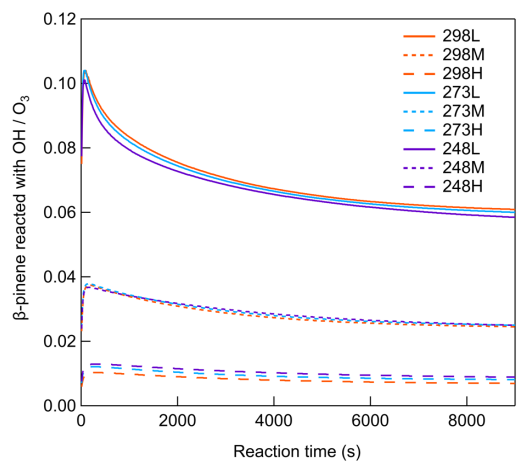


**Figure S3.** Ratio of the accumulated amount of  $\beta$ -pinene reacted with OH versus  $O_3$  for different  $[HO_2]/[RO_2]$  and temperatures (Exp. 298abc, 273abc, 248abc).

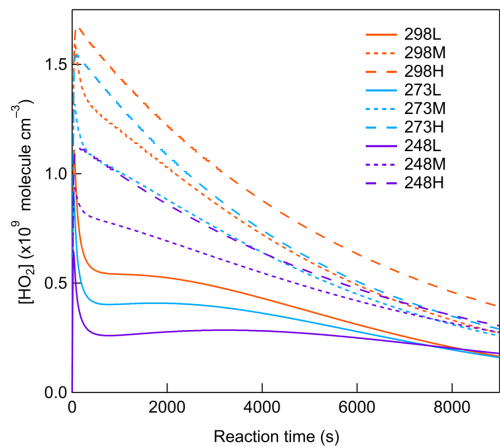
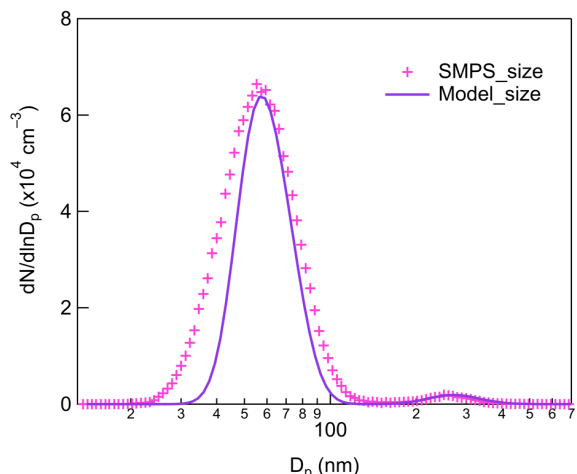
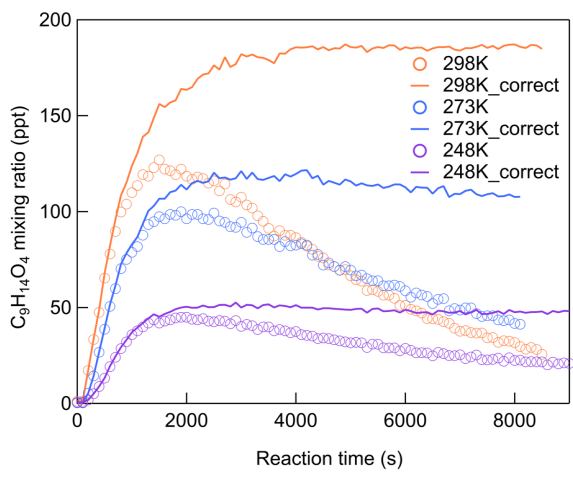


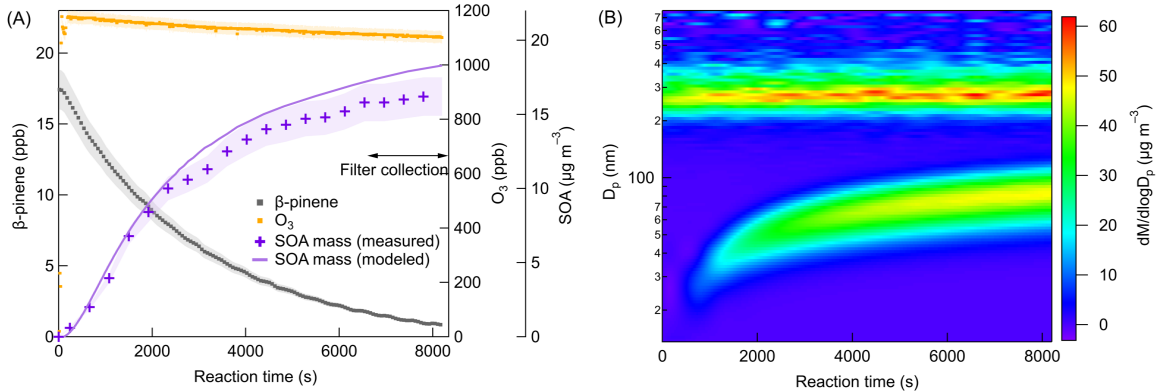
Figure S4. Simulated  $\text{HO}_2$  concentration as a function of reaction time for different  $[\text{HO}_2]/[\text{RO}_2]$  and temperatures (Exp. 298abc, 273abc, 248abc).



**Figure S5.** Particle size distribution from SMPS measurement and COSIMA model result at the end of reaction (Exp. 298a).

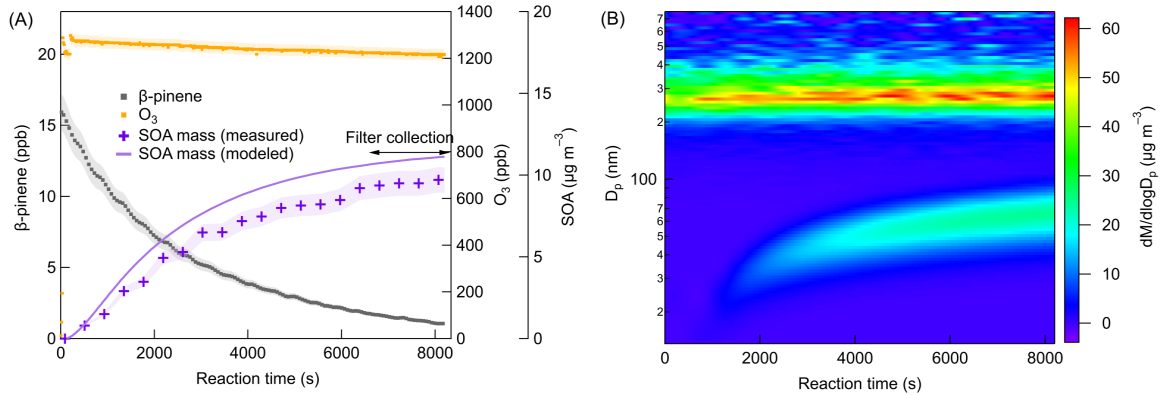


100  
**Figure S6.** Time series of gas-phase  $\text{C}_9\text{H}_{14}\text{O}_4$  mixing ratio before and after wall loss correction at different temperatures (Exp. 298a, 273a, 248a).

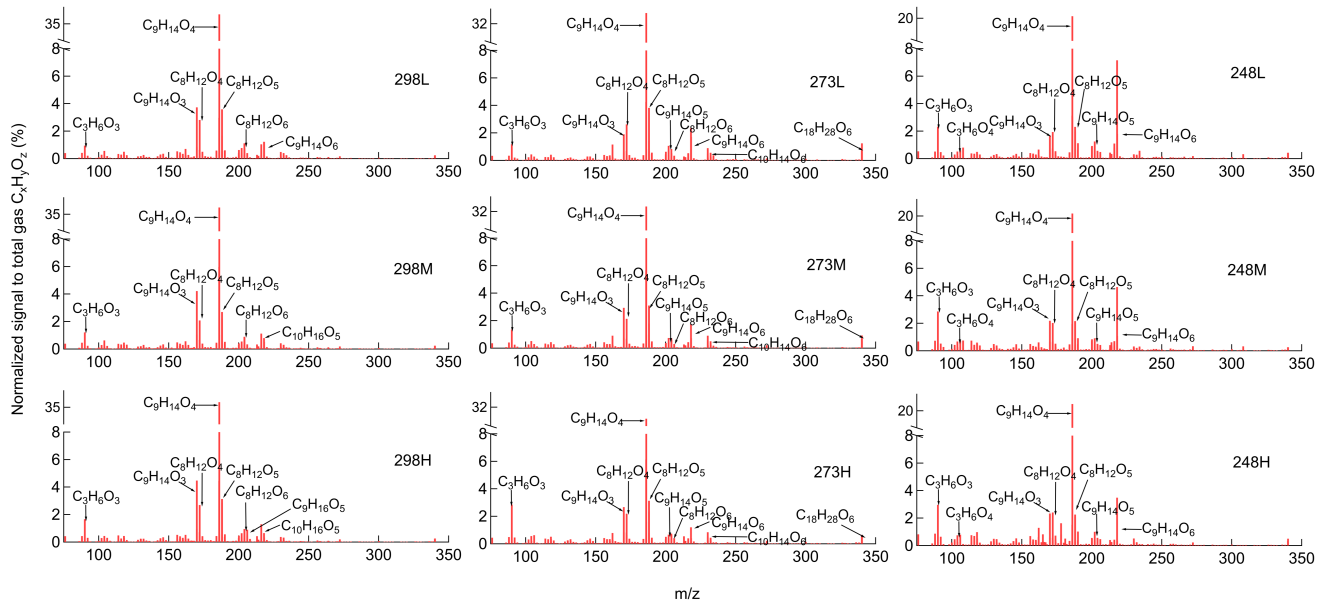


105

**Figure S7.** Time series of (A)  $\beta$ -pinene mixing ratio,  $O_3$  mixing ratio, measured SOA mass concentrations, and simulated SOA mass concentrations after wall loss correction (B) Particle mass size distributions ( $dM/d\log D_p$ ) at 273 K (Exp. 273a).



110 **Figure S8.** Time series of (A)  $\beta$ -pinene mixing ratio,  $O_3$  mixing ratio, measured SOA mass concentrations, and simulated SOA  
mass concentrations after wall loss correction (B) Particle mass size distributions ( $dM/d\log D_p$ ) at 248 K (Exp. 248a).



115 **Figure S9.** The averaged CIMS gas-phase mass spectra for all temperatures at different  $[\text{HO}_2]/[\text{RO}_2]$  (Signals are normalized to total gas  $\text{C}_x\text{H}_y\text{O}_z$ , Exp. 298abc, 273abc, 248abc).

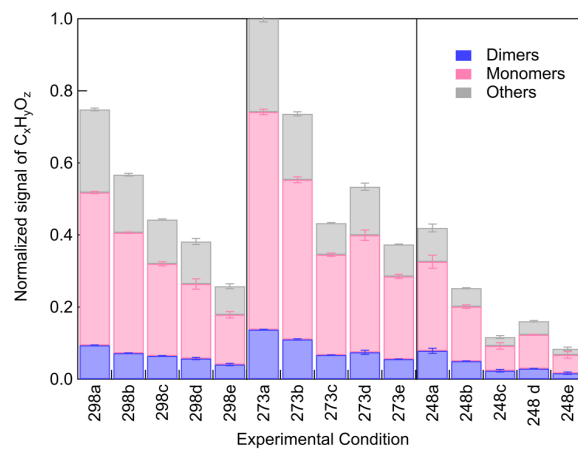
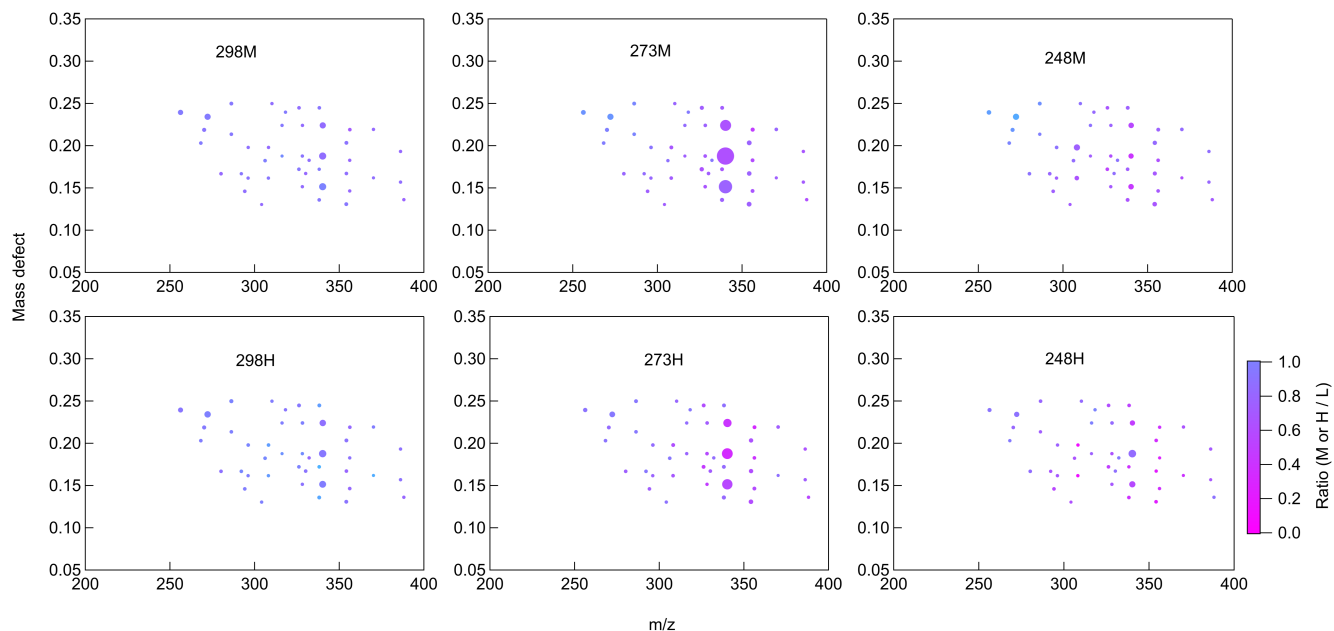


**Figure S10.** Normalized signals of all particle-phase  $C_xH_yO_z$  compounds for different experimental conditions. The other species include  $C_{1-7}$ ,  $C_{11-15}$ , and  $C_{21-29}$  compounds with formulas of  $C_{1-7}H_{2-14}O_{2-9}$ ,  $C_{11-15}H_{12-28}O_{3-11}$ , and  $C_{21-29}H_{30-56}O_{5-12}$ .



125

**Figure S11. Mass defect plots of gas-phase dimers at different temperatures. Markers are sized by the square root of their signals and colored by the ratio of signals at middle and high  $[HO_2]/[RO_2]$  versus signals at low  $[HO_2]/[RO_2]$  at each temperature (Exp. 298bc, 273bc, 248bc).**

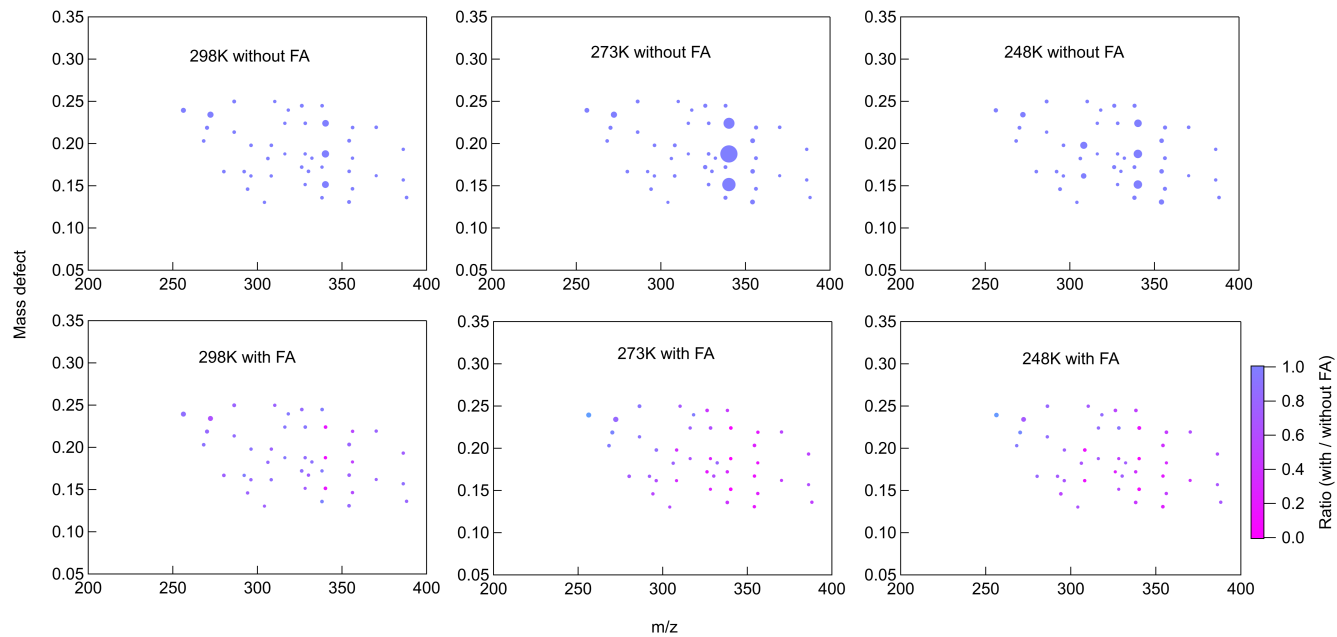


**Figure S12.** Mass defect plots of gas-phase dimers at different temperatures at low  $[HO_2]/[RO_2]$ . Markers are sized by the square root of their signals and colored by the ratio of signals with or without FA versus signals without FA at each temperature (Exp. 298ad, 273ad, 248ad).

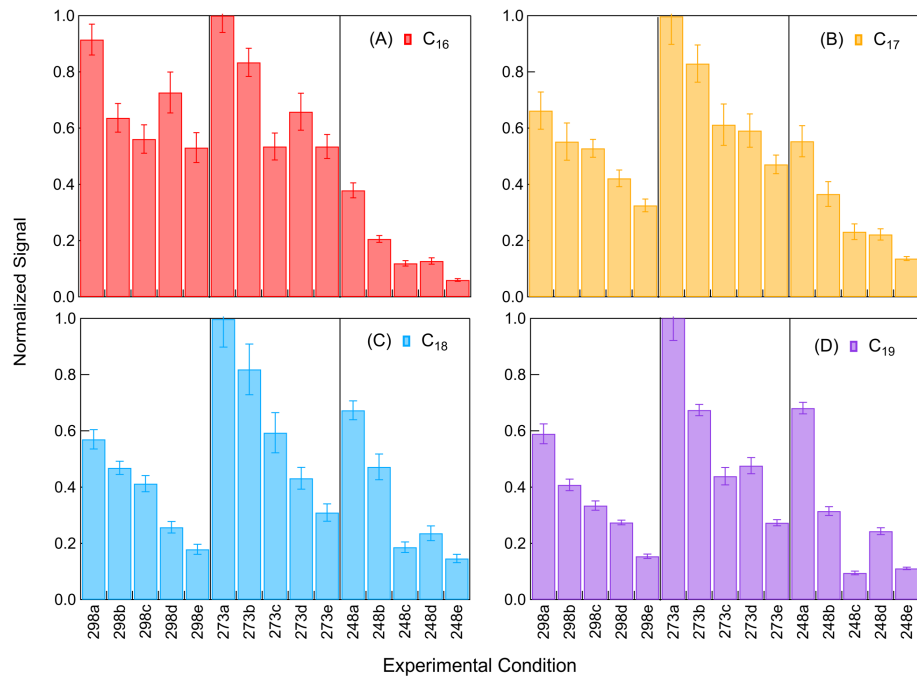


**Figure S13. The particle-phase signals of (A) C<sub>16</sub> (B) C<sub>17</sub> (C) C<sub>18</sub> (D) C<sub>19</sub> dimers normalized to the peak intensity under different experimental conditions.**

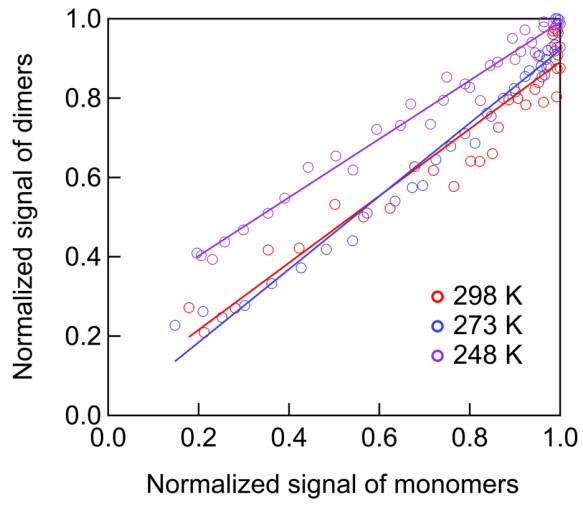
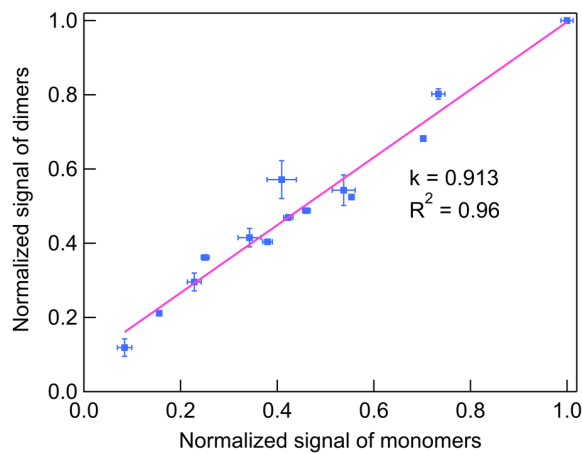
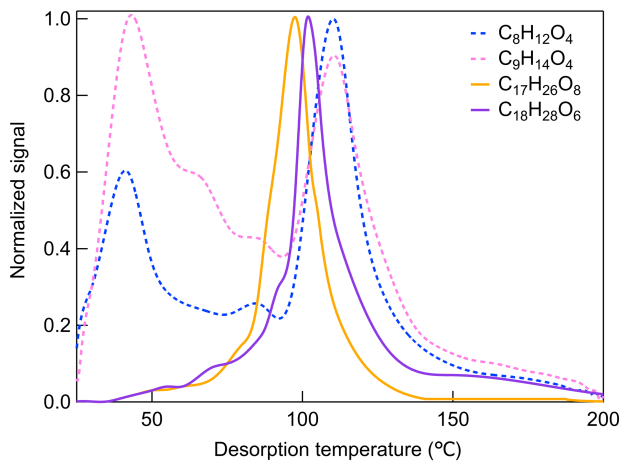


Figure S14. The correlation between gas-phase dimers and monomers at different temperatures (Exp. 298a, 273a, 248a). Solid lines are linear fit with  $R^2$  larger than 0.9.

145

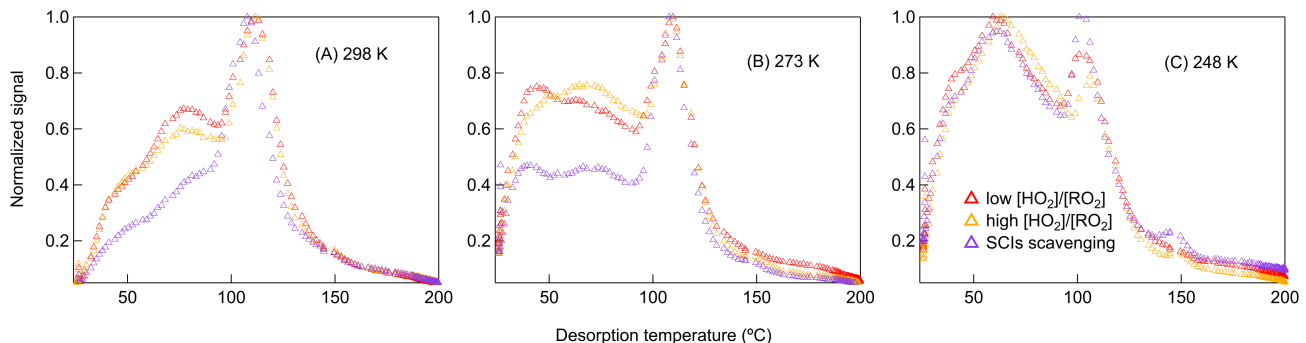


150 **Figure S15.** The correlation between particle-phase normalized signal of dimers with normalized signal of monomers under all conditions. The solid line shows a linear fit.



155

**Figure S16. Thermograms of abundant monomers ( $\text{C}_8\text{H}_{12}\text{O}_4$  and  $\text{C}_9\text{H}_{14}\text{O}_4$ ) and dimers ( $\text{C}_{17}\text{H}_{26}\text{O}_8$  and  $\text{C}_{18}\text{H}_{28}\text{O}_6$ ), i.e., the normalized signals versus desorption temperature.**



160

**Figure S17. Sum thermograms at different temperatures with different  $[HO_2]/[RO_2]$  and SCIs conditions (Exp. 298acd, 273acd, 248acd).**

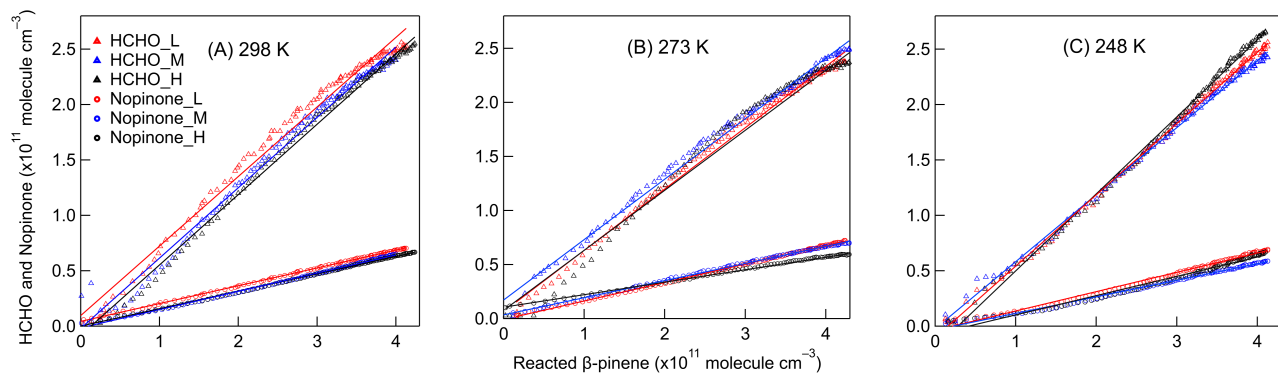


**Figure S18. The formation of formaldehyde (HCHO) and nopinone as a function of  $\beta$ -pinene reacted at 298 K, 273 K, and 248 K for different  $[\text{HO}_2]/[\text{RO}_2]$  (Exp. 298abc, 273abc, 248abc). The lines represent linear fits and  $R^2$  values are larger than 0.95.**

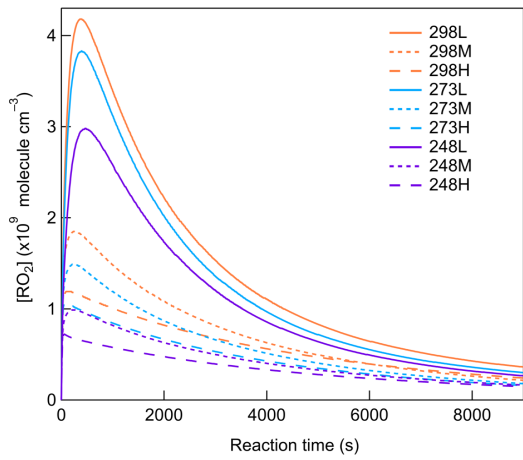


**Figure S19.** Simulated  $\text{RO}_2$  concentration as a function of reaction time for different  $[\text{HO}_2]/[\text{RO}_2]$  and temperatures (Exp. 298abc, 273abc, 248abc).

175

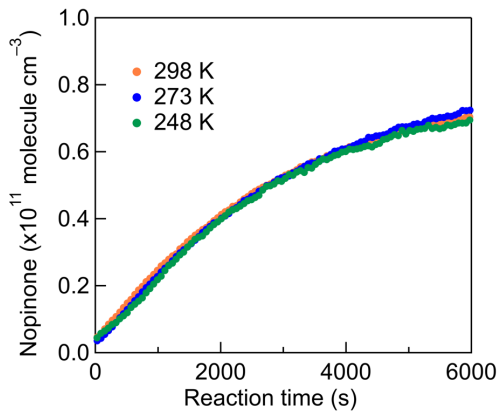


**Figure S20. Time series of nopolone concentration at different temperatures (Exp. 298a, 273a, 248a).**

180

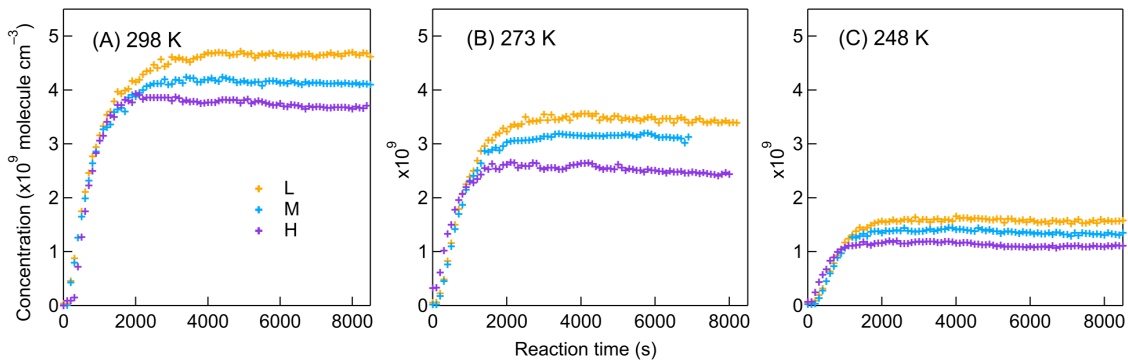


**Figure S21. The impact of  $[\text{HO}_2]/[\text{RO}_2]$  on the gas-phase concentrations of  $\text{C}_9\text{H}_{14}\text{O}_4$  at (A) 298 K (B) 273 K (C) 248 K after wall loss correction (Exp. 298abc, 273abc, 248abc).**

185